Journal of the Optical Society of America A
OPTICS, IMAGE SCIENCE, AND VISION

Analytic calculation of vortex diffraction by a triangular aperture

CHARLOTTE STAHL AND GREG GBUR*

Department of Physics and Optical Science, UNC Charlotte, Charlotte, North Carolina 28223, USA
**Corresponding author: gjgbur@uncc.edu*

Received 1 March 2016; revised 3 May 2016; accepted 4 May 2016; posted 4 May 2016 (Doc. ID 260158); published 25 May 2016

We present an analytic calculation of the diffraction of a vortex beam by a triangular aperture. This calculation is used to study the diffraction of multimode vortex beams and off-axis vortex beams. Implications of these results for the effectiveness of diffraction as a vortex detection method are discussed.

OCIS codes: (050.1960) Diffraction theory; (050.4865) Optical vortices; (260.6042) Singular optics.

http://dx.doi.org/10.1364/JOSAA.33.001175

1. INTRODUCTION

It is now well-known that vortex-like phase structures can manifest in the interference of coherent optical fields or be deliberately imprinted on optical beams. These vortices manifest as lines of zero amplitude in 3D space, about which the phase has a circulating or helical structure. The study of such *optical vortices* and related structures is now its own subfield of optics, known as *singular optics* [1,2].

Optical vortices are known to be stable topological features of a wave field, resistant to perturbations of the amplitude and phase of the field, such as propagation through atmospheric turbulence [3] or obstruction by an obstacle [4]. Furthermore, all vortices have a discrete topological charge m associated with them, defined as the number of cycles by which the phase $\psi(\mathbf{r})$ of the field increases in a closed path C around the singular line, i.e.,

$$m \equiv \frac{1}{2\pi} \oint_C \nabla \psi(\mathbf{r}) \cdot d\mathbf{r}. \tag{1}$$

Because of the continuity of the wave field, the topological charge can only take on integer values.

These two properties—stability and discreteness—have led researchers to consider using vortices as carriers of information, notably in free-space optical communications (see, for instance, [5–7]). However, because the vortex is encoded in the phase structure of the field, new detection techniques are needed in order to efficiently and reliably identify the topological charge, or charges, of a beam. One method that has shown much promise, due to its simplicity and seeming lack of ambiguity, is to diffract the vortex beam by a triangular aperture [8,9]. For a vortex of topological charge m, the diffraction pattern will be a triangular array of bright spots with $|m| + 1$ spots per side; the orientation of the array can be used to deduce the sign of the charge. This method has been shown to work for extremely broadband vortex beams [10] and has been used to facilitate analysis of the birth of new vortices in a so-called fractional vortex beam [11].

In these earlier works, however, the calculations for triangular aperture diffraction have either been done through direct numerical integration or by using only the phase of the field. Furthermore, there seems to be no general research on the properties of vortex diffraction when the beam is nonideal, i.e., when it is off-center from the aperture central axis, or it is a nonpure vortex mode, or both, with the exception of the fractional vortex study mentioned above [11]. Such cases are important to consider for applications like the aforementioned free-space optical communications, in which mode mixing and vortex wander are inevitable.

In this paper, we present an analytic derivation of the diffraction pattern produced by a vortex beam of any order passing through a triangular aperture. This method can take into account the nonideal cases mentioned above. We present examples of the calculation, which we compare with exact numerical results, and discuss the implications of the examples for the use of triangle aperture diffraction in vortex detection. We also note how the calculations here can be extended to calculate the diffraction from a polygonal aperture of any number of sides.

2. VORTEX DIFFRACTION BY A TRIANGULAR APERTURE

We consider the configuration illustrated in Fig. 1. A Laguerre–Gaussian vortex beam is diffracted through an equilateral triangular aperture of side length a, centered on the z axis. We consider the Fraunhofer diffraction of a vortex beam of azimuthal order $\pm m$ ($m \geq 0$) through the aperture; the beam has the following form in the aperture plane:

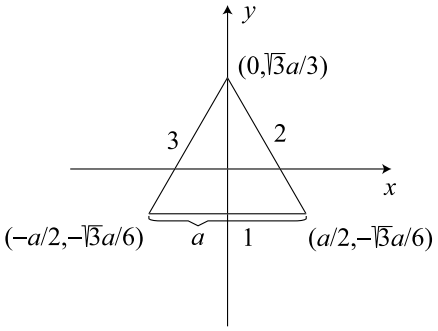

Fig. 1. Illustration of the geometry related to the triangular aperture.

$$U_{\pm m}(x,y)=\frac{[(x-x_0)\pm i(y-y_0)]^m}{w_0^m}, \tag{2}$$

where the center of the vortex is displaced from the origin to location (x_0, y_0). We assume that the beam width w_0 is significantly greater than the size of the aperture a, so that we can neglect the Gaussian envelope of the beam.

Following the earlier phase-only calculations in [8], we treat the diffraction of light as being primarily an edge effect and integrate over the boundary of the triangle. As has been long known, such a geometrical theory of diffraction works well provided the aperture is larger than the wavelength of light [12]. Such an edge diffraction approximation is particularly appropriate for vortex beams, as the center of the vortex is a point of zero amplitude. Unlike the earlier calculations, we explicitly include the amplitude in the integration as well. The total diffracted field may therefore be written in the form

$$U(k_x,k_y)\sim\oint_C\frac{[(x-x_0)\pm i(y-y_0)]^m}{w_0^m}\exp[-i(k_xx+k_yy)]\mathrm{d}l', \tag{3}$$

where C represents the boundary of the triangle, dl' is an infinitesimal path element, and (k_x, k_y) is a transverse wavenumber. This diffracted field may represent the field in the far zone of the aperture or the field in the rear focal plane of a $2f$ focusing system, with the aperture in the front focal plane; we leave off any scaling factors in the integral associated with these specific cases. The integral along each face of the triangle may be represented by a linear parameterization:

$$x=a[\alpha_xt+\beta_x],\qquad y=a[\alpha_yt+\beta_y], \tag{4}$$

with $-1/2\le t\le 1/2$. The constants α_i and β_i will be given for each side of the triangle later in the discussion. Our diffraction integral for a single side then becomes

$$U(k_x,k_y)\sim\gamma\exp[-i\chi a]\int_{-1/2}^{1/2}\frac{[a\alpha t+(a\beta-z_0)]^m}{w_0^m}\exp[-i\kappa at]\mathrm{d}t, \tag{5}$$

with

$$\alpha\equiv\alpha_x\pm i\alpha_y, \tag{6}$$

$$\beta\equiv\beta_x\pm i\beta_y, \tag{7}$$

$$\gamma\equiv a|\alpha|, \tag{8}$$

$$\chi\equiv k_x\beta_x+k_y\beta_y=\mathbf{k}\cdot\boldsymbol{\beta}, \tag{9}$$

$$\kappa\equiv k_x\alpha_x+k_y\alpha_y=\mathbf{k}\cdot\boldsymbol{\alpha}, \tag{10}$$

$$z_0\equiv x_0\pm iy_0. \tag{11}$$

This lengthy list of definitions allows us to evaluate the diffraction effects of all three sides of the triangle with the same notation. To perform the integral, we expand the vortex part of the integrand in binomial form, i.e.,

$$[a\alpha t+(a\beta-z_0)]^m=\sum_{n=0}^m\frac{m!}{n!(m-n)!}(a\alpha t)^n(a\beta-z_0)^{m-n}. \tag{12}$$

We may then write

$$U(k_x,k_y)\sim\frac{\gamma\exp[-i\chi a]}{w_0^m}\sum_{n=0}^m\frac{m!}{n!(m-n)!}(a\beta-z_0)^{m-n}(a\alpha)^n\times\int_{-1/2}^{1/2}t^n\exp[-i\kappa at]\mathrm{d}t. \tag{13}$$

The integral may be evaluated by using the identity

$$\int t^n\exp[ct]\mathrm{d}t=\frac{d^n}{dc^n}\int\exp[ct]\mathrm{d}t, \tag{14}$$

which leads to the expression

$$\int_{-1/2}^{1/2}t^n\exp[-i\kappa at]\mathrm{d}t=\left(\frac{i}{\kappa}\right)^n\frac{d^n}{da^n}j_0(\kappa a/2)\equiv f_n(\kappa,a), \tag{15}$$

where $j_0(x)$ is the zeroth-order spherical Bessel function,

$$j_0(x)=\frac{\sin(x)}{x}. \tag{16}$$

We may finally write

$$U(k_x,k_y)\sim\frac{\gamma\exp[-i\chi a]}{w_0^m}\sum_{n=0}^m\frac{m!}{n!(m-n)!}(a\beta-z_0)^{m-n}(a\alpha)^nf_n(\kappa,a). \tag{17}$$

This expression, with the parameterizations of the three sides of the triangle determined, gives us an analytic expression for the diffraction of a vortex of arbitrary order and center position from a triangular aperture. The parameterizations are readily determined and are given in Table 1.

Equation (17) can be used to quickly evaluate the diffraction pattern of one or more vortex beams superimposed with arbitrary axis positions. However, with some rearrangement, it can also provide qualitative insight into the structure of the diffraction pattern. Such a rearrangement can be performed by use of the generalized Leibniz rule

$$\frac{d^m}{du^m}[f(u)g(u)]=\sum_{n=0}^m\frac{m!}{n!(m-n)!}\frac{d^nf(u)}{du^n}\frac{d^{m-n}g(u)}{du^{m-n}}. \tag{18}$$

Table 1. Coefficients of Parameterization for Each Side of the Triangle

Side	α_x	β_x	α_y	β_y
1	1	0	0	$-\sqrt{3}/6$
2	−1/2	1/4	$\sqrt{3}/2$	$\sqrt{3}/12$
3	−1/2	−1/4	$-\sqrt{3}/2$	$\sqrt{3}/12$

Equation (17) already looks very much like the Leibniz rule and can be adapted to it with some rearrangement. We change the variable of differentiation so that

$$f_n(\kappa, a) = \frac{1}{(a\alpha)^n}\left[\frac{d}{d(-i\kappa/\alpha)}\right]^n j_0(\kappa a/2). \tag{19}$$

On substitution into Eq. (17), we have

$$U(k_x, k_y) \sim \frac{\gamma \exp[-i\chi a]}{w_0^m}\sum_{n=0}^{m}\frac{m!}{n!(m-n)!}(a\beta - z_0)^{m-n} \times \left[\frac{d}{d(-i\kappa/\alpha)}\right]^n j_0(\kappa a/2). \tag{20}$$

Now, we note that

$$(a\beta - z_0)^{m-n} = \exp[i\kappa(a\beta - z_0)/\alpha] \times \left[\frac{d}{d(-i\kappa/\alpha)}\right]^{m-n} \exp[-i\kappa(a\beta - z_0)/\alpha]. \tag{21}$$

On substitution, we may apply the Leibniz rule and write

$$U(k_x, k_y) \sim \frac{\gamma \exp[-i\chi a]}{w_0^m} \exp[i\kappa(a\beta - z_0)/\alpha](i\alpha)^m \times \left[\frac{d}{d\kappa}\right]^m \{\exp[-i\kappa(a\beta - z_0)/\alpha] j_0(\kappa a/2)\}. \tag{22}$$

Here, we have a remarkably concise expression for the diffraction of a vortex by a single edge of a triangular aperture. From it, we may immediately see how the m-lobed triangular diffraction pattern appears for a vortex of order m. A given edge of the triangle will produce a diffraction pattern that varies only in a direction parallel to α, as $\kappa = \mathbf{k}\cdot\boldsymbol{\alpha}$. For the $m = 0$ case, the largest value of $U(k_x, k_y)$ will be at the origin of the function $j_0(\kappa a/2)$; this produces a line perpendicular to $\boldsymbol{\alpha}$ centered on the origin in the diffraction plane, as shown in Fig. 2(a). For the $m = 1$ case, the largest values of $U(k_x, k_y)$ will be the largest values of $d[j_0(\kappa a/2)]/d\kappa$, which will be two lines corresponding with the slopes of the central peak of $j_0(\kappa a/2)$; this is illustrated in Fig. 2(b). Each higher derivative of $j_0(\kappa a/2)$ will introduce another bright line to the diffraction pattern; the $m = 2$ case is shown in Fig. 2(c).

Equation (22) also suggests a crude way to estimate when the displacement of the vortex, characterized by z_0, significantly affects the diffraction pattern. We first note that the peaks of the diffraction pattern will be bounded, at least for low orders, by the first zero of the zeroth-order spherical Bessel function, located at $\kappa a = \pi$; we restrict our attention, then, to this value. We then note that the component of the complex exponential, which includes z_0, will have a small influence when

$$\left|\frac{\kappa z_0}{\alpha}\right| < 1. \tag{23}$$

Substituting the value of κa into this expression, we find a condition on z_0 of the form

$$\left|\frac{z_0}{a}\right| < \frac{|\alpha|}{\pi} = \frac{1}{\pi}. \tag{24}$$

We roughly expect that off-axis effects become significant when $|z_0/a| \sim 0.318$.

We will use the preceding results in the next section to study the off-axis diffraction of vortex beams as well as the diffraction of coherent superpositions. We will continue to use the edge diffraction approximation in these calculations; however, it is to be noted that the complete integral over the aperture can be calculated, though the result is much more complicated. We leave this calculation for Appendix A.

3. CALCULATIONS OF THE DIFFRACTION PATTERN

We return to Eq. (17) for convenience and now use it to investigate the diffraction patterns of vortex beams diffracted by a triangular aperture. In Fig. 3, we first plot the familiar case of on-axis vortex diffraction, i.e., $z_0 = 0$. It can be clearly seen that we reproduce the familiar experimental and theoretical result that the most prominent part of the diffraction pattern is an $m + 1$ lobed triangle, whose orientation depends on the sign of the charge.

We next consider cases in which the vortex core is displaced from the center of the aperture to a position (x_0, y_0). Figure 4 shows the evolution of the diffraction pattern when the vortex center is displaced in the vertical direction. The leftmost intensity spot becomes gradually dimmer, while the right pair gradually coalesce into a single spot. As suggested in the previous section, the case $y_0 = 0.318a$ seems to be the threshold at which the three-lobed pattern is significantly lost. When the vortex core is moved entirely outside the aperture, as in Fig. 4(d), the diffraction pattern is almost identical to the $m = 0$ case; this is to be expected because the field within the aperture in such a case will be almost identical to a tilted plane wave.

Similar observations hold when the vortex center is displaced horizontally, as shown in Fig. 5. Here, the lower right bright intensity spot transforms into the single intensity spot that remains once the vortex center leaves the aperture region.

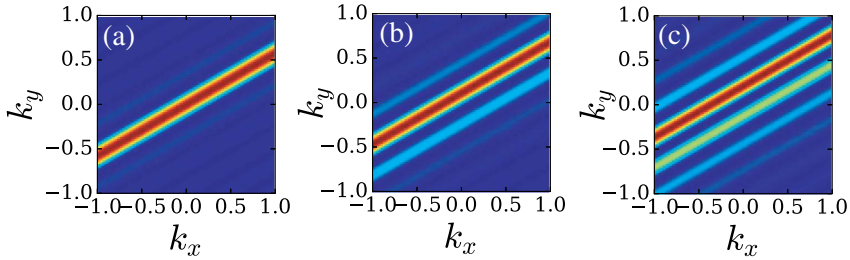

Fig. 2. Bright diffraction lines produced by the second side of the triangular aperture, for (a) $m = 0$, (b) $m = 1$, (c) $m = 2$. We have used $a = 4\lambda$, $w_0 = 2a$.

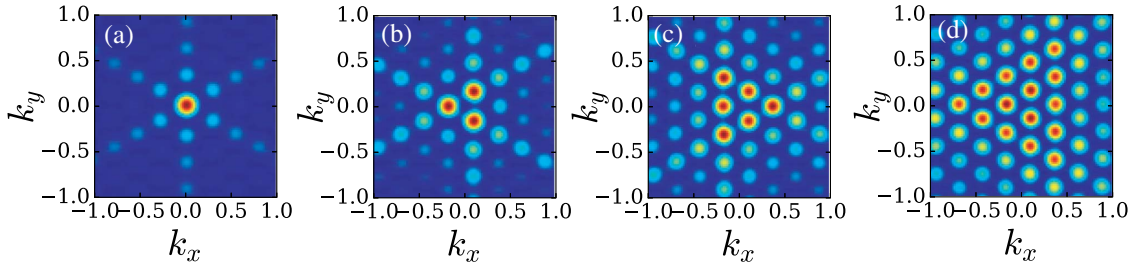

Fig. 3. Diffraction pattern for various vortex orders, with (a) $m = 0$, (b) $m = 1$, (c) $m = -2$, (d) $m = 4$. We have used $a = 4\lambda$, $w_0 = 2a$.

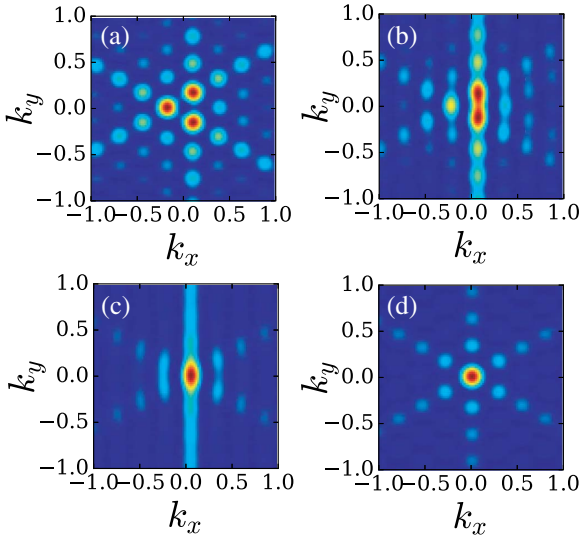

Fig. 4. Diffraction pattern for an $m = 1$ vortex, with $x_0 = 0$ and (a) $y_0 = 0$, (b) $y_0 = 0.318a$, (c) $y_0 = 0.636a$, (d) $y_0 = 2a$. We have used $a = 4\lambda$, $w_0 = 2a$.

Again we see that a displacement of roughly $a/3$ is a threshold at which the three-lobed pattern is lost.

The evolution of the three-lobed pattern into the single-lobed pattern is highly directionally dependent. This suggests that changes in the intensity pattern can be used to determine, and correct, the displacement of the vortex beam. This ability may be useful in applications such as free-space communications, where atmospheric turbulence tends to introduce wandering of an optical beam and any vortices within it.

We also may use our analytic model to investigate the diffraction pattern of a coherent superposition of several modes. Such cases are of interest for two reasons: (1) multimode vortex beams have been proposed as a way to multiplex information; (2) propagation of a pure mode through atmospheric turbulence induces mode mixing. We consider the particular case in which we superimpose an $m = 0$ mode with an $m = 1$ mode, in the form

$$U(x, y) = (1 - b)U_0(x, y) + bU_1(x, y), \tag{25}$$

with b a real-valued weighting parameter. The results of the calculation are shown in Fig. 6. It can be seen that the lower-order mode dominates the diffraction pattern until the amplitude of the higher-order mode is quite large, $b = 0.9$. On reflection, this is understandable because the higher-order modes

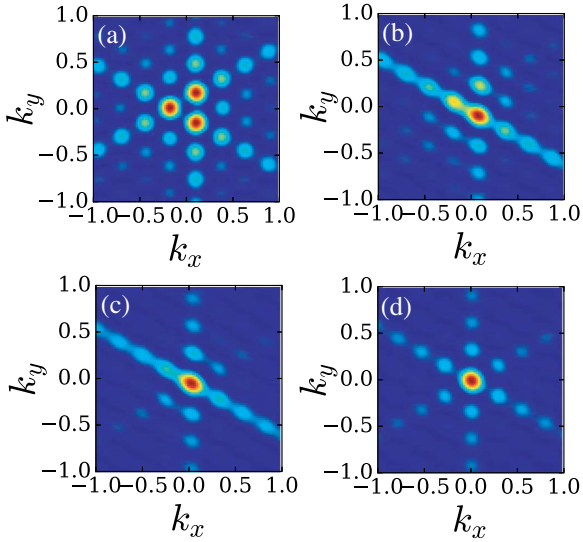

Fig. 5. Diffraction pattern for an $m = 1$ vortex, with $y_0 = 0$ and (a) $x_0 = 0$, (b) $x_0 = 0.318a$, (c) $x_0 = 0.636a$, (d) $x_0 = 2a$. We have again used $a = 4\lambda$, $w_0 = 2a$.

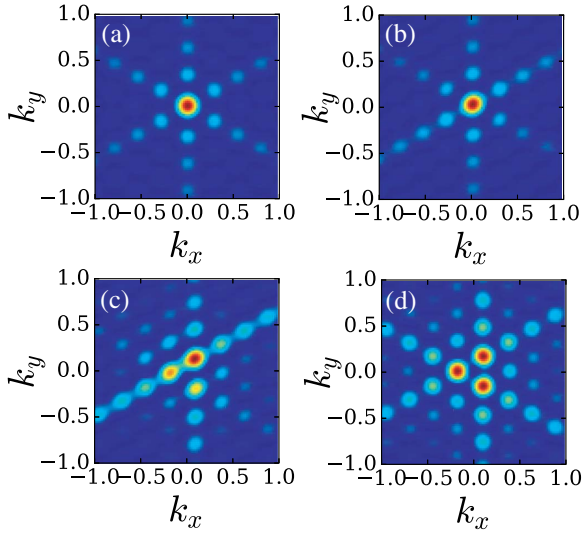

Fig. 6. Diffraction pattern for a mixed-mode beam, with (a) $b = 0$, (b) $b = 0.5$, (c) $b = 0.9$, (d) $b = 1.0$. We have again used $a = 4\lambda$, $w_0 = 2a$.

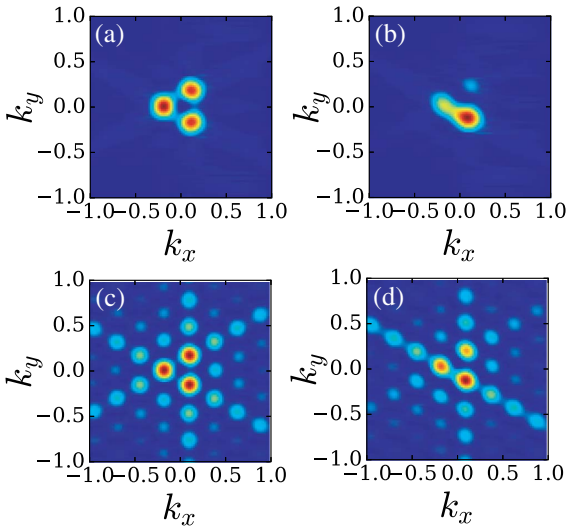

Fig. 7. Comparison of the analytic result with the FFT result, for $m = 1$, $y_0 = 0$, and (a), (c) $x_0 = 0$, FFT and analytic, (b), (d) $x_0 = 0.159a$, FFT and analytic.

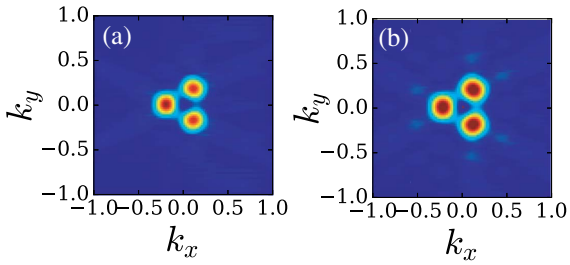

Fig. 8. Comparison of the diffraction pattern of an $m = 1$ vortex from (a) the FFT calculation and (b) the analytic formula, Eq. (A3).

naturally have a smaller intensity near their central axis, resulting in them being dominated by lower-order modes.

It is worth investigating how well the analytic results, which only consider edge diffraction, compare with an exact fast Fourier transform (FFT) calculation of the diffracted field from the full aperture. An example of this comparison is shown in Fig. 7, for horizontal displacement of the vortex center. It can be seen that the primary multispot intensity structure is the same for both methods; however, the large array of secondary spots are not present in the exact result. Furthermore, it appears that the multispot pattern is lost more quickly in the exact result. These results, however, show that the analytic calculation maintains the most important aspects of the diffraction pattern.

4. CONCLUSIONS

We have derived an analytic model for the diffraction of a vortex beam by a triangular aperture and have used this model to provide insight into the nature of the diffraction pattern that arises. The model also allows us to estimate the stability of the vortex diffraction pattern in a number of circumstances, including off-axis beams and mixed-mode beams. Though the system appears to be relatively stable with respect to off-axis deflection of a vortex, it does not appear to be as suitable for mixed-mode beams, as the higher-order modes are generally overwhelmed by the lower-order modes in the diffraction pattern. The results are in good agreement with exact FFT calculations.

It is to be noted that authors have recently considered the diffraction of vortex beams by other polygonal shapes (see, for instance, [13]). Our method readily may be extended to incorporate these cases simply by determining the appropriate parameters α_x, α_y, β_x, and β_y for the apertures in question.

APPENDIX A: COMPLETE INTEGRAL OF VORTEX DIFFRACTION

In this article, we have emphasized the usefulness of our analytic model for understanding the physics of the diffraction pattern and have noted that it provides results that are qualitatively accurate. It is worth noting, though, that it is possible to extend the edge diffraction integral to an integral over an entire area of the triangle, which may be evaluated analytically. The final result is significantly more complicated than the edge case and does not appear to provide the same insight of the simpler model. Furthermore, the process outlined below introduces a removable singularity at $\kappa = 0$, which must be accounted for. For completeness, however, we give the calculation here.

We integrate Eq. (22) over the side length a from 0 to A, where now A is the edge length of the triangular aperture. From the original parameterization, we find that the integral must be multiplied by $\sqrt{3}/6$ in order for the total integral over l and a to cover an area equal to one-third of the total triangle area.

It is to be noted that the derivative of Eq. (22) could be pulled completely outside the integrand if not for the presence of the second exponential from the left. To deal with this, we let $\kappa \to \kappa'$ in that exponent and then take the limit in the end as $\kappa' \to \kappa$, or

$$U(k_x, k_y) \sim \frac{\sqrt{3}}{6}(i\alpha)^m|\alpha|\frac{\partial^m}{\partial\kappa^m}\left\{e^{-i\chi a}e^{i(\kappa'-\kappa)(a\beta-z_0)/\alpha}\frac{\sin(\kappa a/2)}{\kappa/2}\right\}_{\kappa'=\kappa}. \tag{A1}$$

If we write the sine function as complex exponentials, we then have the expression

$$U(k_x, k_y) \sim 2\frac{\sqrt{3}}{6}(i\alpha)^m|\alpha|\frac{\partial^m}{\partial\kappa^m}\left\{e^{-i(\kappa'-\kappa)z_0/\alpha}\frac{e^{-i\chi a}}{\kappa} \times e^{i(\kappa'-\kappa)a\beta/\alpha}\frac{e^{i\kappa a/2}-e^{-i\kappa a/2}}{2i}\right\}_{\kappa'=\kappa}. \tag{A2}$$

Now the variable a only appears in complex exponents. We may readily integrate with respect to a to find

$$U(k_x, k_y) \sim a\frac{\sqrt{3}}{6}(i\alpha)^m|\alpha|\frac{\partial^m}{\partial\kappa^m}\left\{\frac{e^{-i(\kappa'-\kappa)z_0/\alpha}}{i\kappa} \times [e^{i\delta_+}j_0(\delta_+) - e^{i\delta_-}j_0(\delta_-)]\right\}_{\kappa'=\kappa}, \tag{A3}$$

where, for convenience, we have introduced

$$\delta_\pm \equiv a[-\chi + (\kappa'-\kappa)\beta/\alpha \pm \kappa/2]/2. \tag{A4}$$

Each side of the triangle may be treated in the same manner to derive the total field. For small values of m, the derivatives may

be calculated analytically and the limit $\kappa' \to \kappa$ taken to get the final result.

A comparison between the exact FFT result and results derived from Eq. (A3) is shown in Fig. 8. We see excellent quantitative and qualitative results.

Funding. Air Force Office of Scientific Research (AFOSR) (FA9550-13-1-0009).

REFERENCES

1. M. Soskin and M. Vasnetsov, "Singular optics," in *Progress in Optics*, E. Wolf, ed. (Elsevier, 2001), vol. **42**, p. 219.
2. M. Dennis, K. O'Holleran, and M. Padgett, "Singular optics: Optical vortices and polarization singularities," in *Progress in Optics*, E. Wolf, ed. (Elsevier, 2009), vol. **53**, p. 293.
3. G. Gbur and R. Tyson, "Vortex beam propagation through atmospheric turbulence and topological charge conservation," J. Opt. Soc. Am. A **25**, 225–230 (2008).
4. M. Vasnetsov, I. Marienko, and M. Soskin, "Self-reconstruction of an optical vortex," J. Exp. Theor. Phys. Lett. **71**, 130–133 (2000).
5. G. Gibson, J. Courtial, M. Padgett, M. Vasnetsov, V. Pas'ko, S. Barnett, and S. Franke-Arnold, "Free-space information transfer using light beams carrying orbital angular momentum," Opt. Express **12**, 5448–5456 (2004).
6. J. Wang, J.-Y. Yang, I. Fazal, N. Ahmed, Y. Yan, H. Huang, Y. Ren, Y. Yue, S. Dolinar, M. Tur, and A. Willner, "Terabit free-space data transmission employing orbital angular momentum multiplexing," Nat. Photonics **6**, 488–496 (2012).
7. M. Krenn, R. Fickler, M. Fink, J. Handsteiner, M. Malik, T. Scheidl, R. Ursin, and A. Zeilinger, "Communication with spatially modulated light through turbulent air across Vienna," New J. Phys. **16**, 113028 (2014).
8. J. Hickmann, E. Fonesca, W. Soares, and S. Chávez-Cerda, "Unveiling a truncated optical lattice associated with a triangular aperture using light's orbital angular momentum," Phys. Rev. Lett. **105**, 053904 (2010).
9. L. de Araujo and M. Anderson, "Measuring vortex charge with a triangular aperture," Opt. Lett. **36**, 787–789 (2011).
10. M. Anderson, H. Bigman, L. de Araujo, and J. Chaloupka, "Measuring the topological charge of ultrabroadband optical-vortex beams with a triangular aperture," J. Opt. Soc. Am. B **29**, 1968–1976 (2012).
11. A. Mourka, C. Shanor, K. Dholakia, and E. Wright, "Visualization of the birth of an optical vortex using diffraction from a triangular aperture," Opt. Express **19**, 5760–5771 (2011).
12. J. Keller, "Geometrical theory of diffraction," J. Opt. Soc. Am. **52**, 116–130 (1962).
13. Y. Liu, S. Sun, J. Pu, and B. Lü, "Propagation of an optical vortex beam through a diamond-shaped aperture," Opt. Laser Technol. **45**, 473–479 (2013).